Static Stiffness Modeling and Sensitivity Analysis for Geared System Used for Rotary Feeding

Lin Han, Dawei Zhang, Yanling Tian, Fujun Wang and Hui Xiao
Key Lab of Ministry of Education for Mechanism Theory and Equipment Design, Tianjin University, Tianjin 300072, China

Abstract. The positioning accuracy of rotary feed system under load greatly depends on the static stiffness of mechanical transmission system. This paper proposes a unified static stiffness model of rotary feed system with geared transmission system. Taking the torsional stiffness of transmission shaft, mesh stiffness of gear pairs into account, the motion equations of the whole transmission system are presented. Based on the static equilibrium, a unified expression for the relationship between torsional angles of two adjacent elements is derived. Then a unified static stiffness model is presented. Furthermore, analytical expressions for sensitivity analysis of the static stiffness on the individual element's stiffness and design parameters are derived. The presented model is verified by a traditional model, and a good agreement is obtained. The influence of phase angle of meshing gear pairs on the resultant static stiffness is investigated. An example transmission system is employed to perform the sensitivity analysis and the results are analyzed. The proposed model provides an essential tool for the design of rotary feed system satisfying requirement of static stiffness.

Key words: rotary feeding; geared system; static equilibrium; static stiffness; sensitivity analysis.

1. Introduction

Besides the linear feed system, rotary feed system, as a key component of multi-axis machine tool, plays a significant role in the performance of a whole machine tool. It’s known that transmission chain with weak stiffness will degrade the positioning accuracy of the rotary feeding. And stick-slip may be easily introduced if the stiffness of the transmission does not satisfy the requirement. Wu et al.[1] proposed a mathematical model for the stiffness of the linear feed system of a heavy duty lathe. Ebrahimi M and Whalley R.[2] modeled the stiffness of feed drive system of a machine tool, and then analyzed the effect of back-lash in transmission train and cutting force to the response of the system. Kim and Chung[3] also modeled stiffness of a ball screw feed drive system where the motor is directly connected to the screw, then analyzed the influences of parameters of controller on the system stability.

Most of literature about rotary feeding is about the geometric error measurement and modeling. W.T. Lei et al.[4] proposed a measurement method for the geometric error of a rotary axis by double ball-bar. M. TSUTSUMI et al.[5] measured and compared the characteristics of two rotary tables driven by worm gear and roller gear cam, and the results showed a better performance of the kind of table with roller gear cam. Hong et al.[6,7] investigated the influence of position-dependent geometric errors of rotary axes on a machining test of cone frustum by five-axis machine tools through both simulation and experiment approaches. After sensitivity analysis, the results showed that not all of the geometric error components of the table’s are the critical effort factors for cone frustum machining test. Later, the authors presented a method for observing thermally induced geometric errors of a rotary axis with a static R-test. The thermal influence on the error motions of a rotary axis is quantitatively parameterized by geometric errors that vary with time. Ibaraki et al.[8,9] proposed a scheme to calibrate error motions of rotary axes on a five-axis machining center by using the R-test and an algorithm to identify both location errors and position-dependent geometric errors were also presented, after which, a scheme to calibrate the error map of rotary axes by on-the-machine measurement of test pieces by using a contact-type touch-trigger probe installed on the machine's spindle was also proposed. K. Lee et al.[10,11] proposed a method to measure the geometric errors of the rotary axis of machine tools by double ball-bar, where set-up errors were also taken into account in the measured data. Then an error separation technology by polynomial fitting was employed to get the individual error terms. Recently, the measurement uncertainty analysis was performed to quantify the confidence interval of the result.

The research about dynamic performance of rotary feed system could be found in references [12-17]. M.S. Lysov, A.V. Starikov[12] modeled the nonlinear factors involved in worm geared system and implemented a simulation incorporating the controller part. The results showed that the free play in the kinematic chain and the stiffness of the mechanical transmission had a direct effect on the static and dynamic precision of the table's control system. Ryuta SATO[13] proposed a mathematical model of CNC rotary table driven by a worm gear, where the inertia of motor, spur and worm gears were incorporated. The simulation results agreed well with those from the experiment. A fault diagnosis theme for rotary axis used in machine tools was proposed by F. Zhao et al., based on a motor current test and the ensemble empirical mode decomposition method[14]. The authors in [15] investigated the axial performance of a large and heavy NC rotary table, based on the force analysis of a ZT20SW driven by double worm gear pairs. A dynamic model and an electromechanical-hydraulic coupling model in the circumferential direction were established. Then the factors affecting the dynamic accuracy of the table were revealed. Later, the preload of the brake worm employed in an NC rotary table was optimized by modeling an electromechanical-hydraulic coupling [16]. Feng and Jiang[17] proposed a type of rotary feed system supplied by a constant flow pump and a constant pressure one to satisfy the higher stiffness requirement in heavy machine tools. Then a mathematical model is presented based on hydrostatic theory to predict the axial static performance of the rotary table.

The positioning accuracy of the rotary feed system without load mainly depends on the geometric error (e.g., free play between meshing teeth); however, when torque load is applied, rotating angular deviation from the desired mainly comes from the stiffness of the transmission chain. However, few researches could have been found.

The purposes of this paper include: (1) modeling the stiffness of a power train employed in rotary feed system of a multi-axis machine tool in a unified way; (2) conducting sensitivity analysis of the equivalent stiffness. Firstly, the definition of the static stiffness in power chain is given. Then a unified static stiffness model is proposed based on static equilibrium condition of the chain. The analytical expressions for sensitivity analysis of the equivalent stiffness to the individual stiffness are then derived. Furthermore, the sensitivity to the design parameters of components of the power train is also presented. Finally, a case study is conducted.

2. Static Stiffness Modeling

A typical geared transmission system is shown in Figure 1. T_1 is the driving torque, T_L is the load torque, θ_i (i=1, … , N+1) represent rotating angle of each element in the transmission chain. Usually, a transmission chain includes motor, belt, gear pairs and shafts, et al.

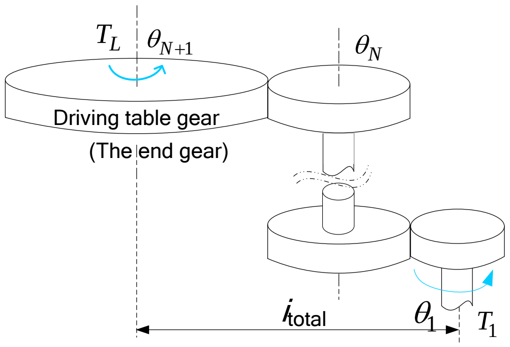

Figure 1 a typical geared transmission system

Under rigid body assumption, the ideal transmission ratio from the driving to the end gear or worktable is i_{total}, that's to say $\theta_{N+1} = i_{total}\theta_1$. However, because of the elasticity of shaft and meshing teeth, the actual rotating angle of the end gear or driving table gear is

$$\theta_{N+1} = i_{total}\theta_1 + \Delta\theta \tag{1}$$

where $\Delta\theta$ is the equivalent total torsional deflection of the geared transmission due to the elastic deformations of shaft and meshing gear pairs.

A schematic diagram of the transmission chain with elastic shaft and meshing teeth is shown in Figure 2(a) where the shaft is regarded as a mass-less elastic element and the inertia is equally distributed to its two ends. If a load torque T_L is applied to the worktable, then the static stiffness of the transmission chain could be given as

$$k_{static} = \frac{T_L}{\theta_{N+1} - i_{total}\theta_1} = \frac{T_L}{\Delta\theta} \tag{2}$$

The rotation angle of each element is denoted as θ_i in sequence. The even subscript represents the driving gear, whereas the odd represents the driven gear. Similarly, the odd subscript numbers of k_i represent the torsional stiffness of the $(i\text{-}2)^{th}$ shaft, and the even ones stand for the meshing stiffness of gear pairs.

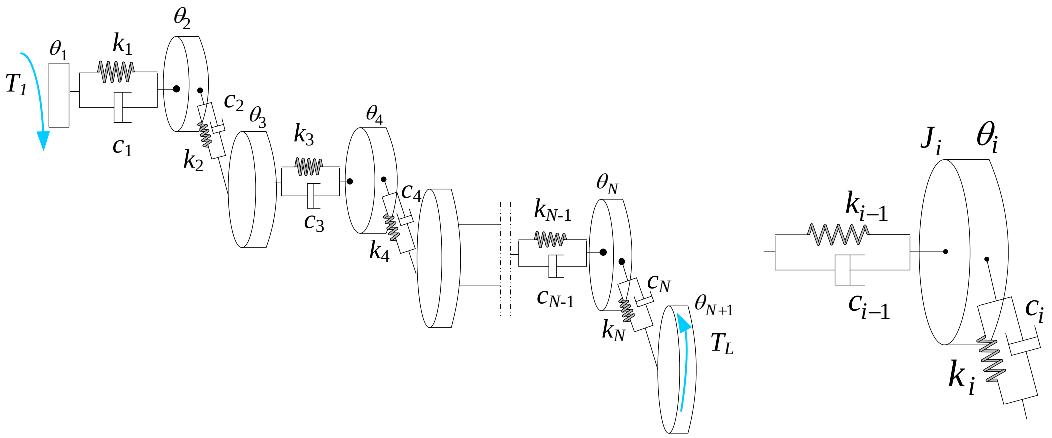

(a) (b)

Figure 2 schematic diagram of the transmission chain

A free body diagram of a gear is shown in Figure 2(b). According to the second law of Newton, the dynamic equation of the transmission system could be obtained:

$$\begin{aligned}
&J_1\ddot{\theta}_1(t) + c_1\dot{q}_1(t) + k_1 q_1(t) = T_1(t) \\
&J_2\ddot{\theta}_2(t) - c_1\dot{q}_1(t) - k_1 q_1(t) + r_{b2}c_2\dot{q}_2(t) + r_{b2}k_2 q_2(t) = 0 \\
&J_3\ddot{\theta}_3(t) - r_{b3}c_2\dot{q}_2(t) - r_{b3}k_2 q_2(t) + c_3\dot{q}_3(t) + k_3 q_3(t) = 0 \\
&\vdots \\
&J_N\ddot{\theta}_N(t) - c_{N-1}\dot{q}_{N-1}(t) - k_{N-1}q_{N-1}(t) + r_{bN}c_N\dot{q}_N(t) + r_{bN}k_N q_N(t) = 0 \\
&J_{N+1}\ddot{\theta}_{N+1}(t) - r_{b(N+1)}c_N\dot{q}_N(t) - r_{b(N+1)}k_N q_N(t) = T_L(t)
\end{aligned} \tag{3}$$

where $q_n(t) = \begin{cases} \theta_n(t) - \theta_{n+1}(t) & n = odd \\ r_{bn}\theta_n(t) - r_{b(n+1)}\theta_{n+1}(t) & n = even \end{cases}$, $J_n\,(n = 1,\ldots,N+1)$ represent inertia of each gear, r_{bi} denotes the radius of basis circle of i^{th} gear and c_i means the damping coefficients of both shafts and meshing gears.

Under static equilibrium condition, there are no relative movements between elements, which means both the rotating speeds and accelerations of each element in the transmission system are zeros:

$$\dot{\theta}_1 = \dot{\theta}_2 = \cdots = \dot{\theta}_N = \dot{\theta}_{N+1} = 0, \ \ddot{\theta}_1 = \ddot{\theta}_2 = \cdots = \ddot{\theta}_N = \ddot{\theta}_{N+1} = 0 \qquad (4)$$

Then Eq.(3) could be simplified as

$$\begin{aligned}
&k_1 q_1(t) = T_1(t) \\
&-k_1 q_1(t) + r_{b2} k_2 q_2(t) = 0 \\
&-r_{b3} k_2 q_2(t) + k_3 q_3(t) = 0 \\
&\vdots \\
&-k_{N-1} q_{N-1}(t) + r_{bN} k_N q_N(t) = 0 \\
&-r_{b(N+1)} k_N q_N(t) = T_L(t)
\end{aligned} \qquad (5)$$

Assuming that the motor shaft is fixed ($\theta_1 = 0$) and substituting expressions of $q_n(t)$ into above equations yields

$$\begin{aligned}
&\theta_1(t) = 0 \\
&\theta_2(t) = \frac{r_{b2} r_{b3} k_2}{k_1 + r_{b2}^2 k_2} \theta_3(t) = A_{23} \theta_3(t) \\
&\theta_3(t) = \frac{k_3}{k_3 + r_{b3}^2 k_2 - r_{b2} r_{b3} k_2 A_{23}} \theta_4(t) = A_{34} \theta_4(t) \\
&\vdots \\
&\theta_N(t) = A_{N(N+1)} \theta_{N+1}(t)
\end{aligned} \qquad (6)$$

where $A_{n(n+1)}$ takes the following general form

$$A_{n(n+1)} = \begin{cases} \dfrac{k_n}{k_n + r_{bn}^2 k_{(n-1)} - r_{b(n-1)} r_{bn} k_{(n-1)} A_{(n-1)n}} & n = odd \\[2ex] \dfrac{r_{bn} r_{b(n+1)} k_n}{k_{(n-1)} + r_{bn}^2 k_n - k_{(n-1)} A_{(n-1)n}} & n = even \end{cases} \qquad (7)$$

To be noted that $A_{12} = 0$. Recalling the last equation of Eq. (5), the general expression for static stiffness is obtained:

$$k_{static} = \frac{T_L}{\Delta\theta} = r_{b(N+1)}^2 k_N - r_{bN} r_{b(N+1)} k_N A_{N(N+1)} \tag{8a}$$

As the meshing stiffness of gear pairs is time-varying, the above equation could be rewritten as

$$k_{static}(t) = r_{b(N+1)}^2 k_N - r_{bN} r_{b(N+1)} k_N A_{N(N+1)} \tag{8b}$$

which is called quasi-static stiffness of the transmission system.

3. Sensitivity Analysis

3.1 Sensitivity to element's stiffness

To find the most sensitive stiffness element to the equivalent tangential stiffness in the transmission system, sensitivity analysis is conducted in this section. The results of sensitivity analysis could be employed to find the element with low stiffness and then make modifications to satisfy the stiffness requirement of the whole transmission chain.

As could be seen from Eq. (7), k_n is related to both $A_{n(n+1)}$ and $A_{(n+1)(n+2)}$. Differentiating k_{static} with respect to k_n yields

$$\frac{\partial k_{static}}{\partial k_n} = \frac{\partial k_{static}}{\partial A_{N(N+1)}} \frac{\partial A_{N(N+1)}}{\partial A_{(N-1)N}} \cdots \frac{\partial A_{(n+2)(n+3)}}{\partial A_{(n+1)(n+2)}} \mathring{A}_{n+1}(k_n) \tag{9}$$

where $\mathring{A}_{n+1}(k_n) = \frac{\partial A_{(n+1)(n+2)}}{\partial k_n} + \frac{\partial A_{(n+1)(n+2)}}{\partial A_{n(n+1)}} \cdot \frac{\partial A_{n(n+1)}}{\partial k_n}$,

According to Eq.(7), if n is an odd number, then n+1 is an even one and there are

$$\frac{\partial A_{n(n+1)}}{\partial A_{(n-1)n}} = \frac{r_{b(n-1)} r_{bn} k_{(n-1)} A^2{}_{n(n+1)}}{k_n} \tag{10-a}$$

$$\frac{\partial A_{(n+1)(n+2)}}{\partial k_n} = \frac{(A_{n(n+1)} - 1) A_{(n+1)(n+2)}^2}{r_{b(n+1)} r_{b(n+2)} k_{n+1}} \tag{10-b}$$

$$\frac{\partial A_{n(n+1)}}{\partial k_n} = \frac{A_{n(n+1)}(1 - A_{n(n+1)})}{k_n} \tag{10-c}$$

Similarly, there are

$$\frac{\partial A_{n(n+1)}}{\partial A_{(n-1)n}} = \frac{k_{(n-1)} A^2{}_{n(n+1)}}{r_{bn} r_{b(n+1)} k_n} \tag{11-a}$$

$$\frac{\partial A_{(n+1)(n+2)}}{\partial k_n} = -\frac{(r_{bn+1}^2 - r_{bn} r_{b(n+1)} A_{n(n+1)}) A_{(n+1)(n+2)}^2}{k_{n+1}} \tag{11-b}$$

$$\frac{\partial A_{n(n+1)}}{\partial k_n} = \frac{A_{n(n+1)}(r_{bn+1} - r_{bn} A_{n(n+1)})}{k_n r_{bn+1}} \tag{11-c}$$

If n is an even number.

Thus, the expression for $\mathring{A}_{n+1}(k_n)$ is given by

$$\mathring{A}_{n+1}(k_n) = \begin{cases} \dfrac{-(A_{n(n+1)} - 1)^2 A_{(n+1)(n+2)}^2}{r_{bn+1} r_{bn+2} k_{n+1}} & n = odd \\ \dfrac{-(r_{bn} A_{n(n+1)} - r_{bn+1})^2 A_{(n+1)(n+2)}^2}{k_{n+1}} & n = even \end{cases} \tag{12}$$

And the partial differential of k_{static} to $A_{(n+1)(n+2)}$ is

$$\frac{\partial k_{static}}{\partial A_{(n+1)(n+2)}} = \begin{cases} -r_{bn+1} r_{bn+2} k_{n+1} \prod_{i=n+2}^{N} A^2{}_{i(i+1)} & n = odd, n \le N-2 \\ -k_{n+1} \prod_{i=n+2}^{N} A^2{}_{i(i+1)} & n = even, n \le N-2 \\ -r_{bN} r_{bN+1} k_N & n = N-1 \end{cases} \tag{13}$$

Combining equations (9)~(13), the sensitivity formulation of static stiffness to stiffness of each element could be obtained:

$$\frac{\partial k_{static}}{\partial k_n}=\begin{cases}(A_{n(n+1)}-1)^2\prod_{i=n+1}^{N}A^2{}_{i(i+1)} & n=odd, n\le N-1\\(r_{bn}A_{n(n+1)}-r_{bn+1})^2\prod_{i=n+1}^{N}A^2{}_{i(i+1)} & n=even, n\le N-1\\(r_{bN}A_{N(N+1)}-r_{bN+1})^2 & n=N\end{cases} \tag{14}$$

where n=odd represents the sensitivity to shaft's torsional stiffness, while n=even stands for the sensitivity to the mesh stiffness of gear pairs.

3.2 Sensitivity to shaft's parameters

In the above section, the sensitivity to element's stiffness is analyzed. However, to facilitate the design of transmission system, the relationship between the static stiffness and design parameters has to be established, which introduces the sensitivity analysis of static stiffness to design parameters. Thus, in this section, the influences of design parameters (radius and length of a shaft, teeth number and module of gears, etc) on the static stiffness will be investigated.

As shown in Figure 3, the torsional stiffness of ith section of the nth shaft could be expressed as

$$k_n^{(i)}=GJ^{(i)}/L^{(i)} \tag{15-a}$$

where $G=0.5E/(1+v)$, E being the Young modulus, v the Poisson coefficient, respectively; $L^{(i)}$ is the length of the ith section, $J_n^{(i)}=\pi r_n^{(i)4}/2$ is the polar moment of inertia of the section, $r_n^{(i)}$ is radius of i^{th} section of n^{th} shaft.

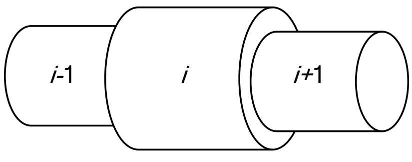

Figure 3 schematic of shaft in transmission system

The torsional stiffness of the nth shaft could be regarded as a series of these sections, and could be computed as

$$k_n = [\sum_{i=1}^{N} 1/k_n^{(i)}]^{-1} \tag{15-b}$$

or

$$k_n = \frac{\prod_{i=1}^{S_n} k_n^{(i)}}{D_n(S_n)} \tag{15-c}$$

where $D_n(S_n) = \prod_{i=2}^{S_n} k_n^{(i)} + \prod_{i=1, i\neq 2}^{S_n} k_n^{(i)} + \prod_{i=1, i\neq 3}^{S_n} k_n^{(i)} + \text{L} + \prod_{i=1, i\neq S-1}^{S_n} k_n^{(i)} + \prod_{i=1}^{S_n-1} k_n^{(i)}$.

Seen from Eq. (15a), differentiating $k_n^{(i)}$ with respect to $r_n^{(i)}$ yields

$$\frac{\partial k_n^{(i)}}{\partial r_n^{(i)}} = \frac{2G\pi r_n^{(i)3}}{L_n^{(i)}} \tag{16-a}$$

Similarly, the partial differential to the length is computed as

$$\frac{\partial k_n^{(i)}}{\partial L_n^{(i)}} = -\frac{G\pi r_n^{(i)4}}{2L_n^{(i)2}} \tag{16-b}$$

Combining Eqs.(15) &(16), the sensitivity of the nth torsional stiffness to the shaft's parameters is given by

$$\frac{\partial k_n}{\partial r_n^{(j)}} = \frac{\partial k_n}{\partial k_n^{(j)}} \cdot \frac{\partial k_n^{(j)}}{\partial r_n^{(j)}} = \frac{H_n^{(j)}}{D_n(S_n)^2} \cdot (\frac{2G\pi r_n^{(i)3}}{L_n^{(i)}}) \tag{17-a}$$

$$\frac{\partial k_n}{\partial L_n^{(j)}} = \frac{\partial k_n}{\partial k_n^{(j)}} \cdot \frac{\partial k_n^{(j)}}{\partial L_n^{(j)}} = \frac{H_n^{(j)}}{D_n(S_n)^2} \cdot (-\frac{G\pi r_n^{(i)4}}{2L_n^{(i)2}}) \tag{17-b}$$

where

$$\begin{aligned} H_n^{(j)} = D_n(S_n) \prod_{i=1, i\neq j}^{S_n} k_n^{(i)} - \prod_{i=1}^{S_n} k_n^{(i)} (\prod_{i=2, i\neq j}^{S_n} k_n^{(i)} + \prod_{i=1, i\neq 2, i\neq j}^{S_n} k_n^{(i)} + \text{L} + \prod_{i=1, i\neq j-1, i\neq j}^{S_n} k_n^{(i)} \\ + \prod_{i=1, i\neq j+1, i\neq j}^{S_n} k_n^{(i)} + \text{L} + \prod_{i=1, i\neq j, i\neq S_n-1}^{S_n} k_n^{(i)} + \prod_{i=1, i\neq j}^{S_n-1} k_n^{(i)}) \end{aligned} .$$

Further, the sensitivity of the static stiffness to the design parameters of shafts could be obtained:

$$\frac{\partial k_{static}}{\partial r_n^{(j)}} = -\frac{H_n^{(j)}}{(D_n(S_n))^2} \cdot \frac{16L_n^{(j)}}{\pi G r_n^{(j)5}} \cdot (A_{n(n+1)} - 1)^2 \prod_{i=n+1}^{N} A^2{}_{i(i+1)} \tag{18-a}$$

$$\frac{\partial k_{static}}{\partial L_n^{(j)}} = \frac{H_n^{(j)}}{(D_n(S_n))^2} \cdot \frac{4}{\pi G r_n^{(j)4}} \cdot (A_{n(n+1)} - 1)^2 \prod_{i=n+1}^{N} A^2{}_{i(i+1)} \tag{18-b}$$

Here, to be noted that *n* must be an odd number corresponding to the stiffness of shaft.

3.3 Sensitivity to gear's parameters

The meshing stiffness of gear pair is determined by gear's parameters, like the teeth number z, module *m*, width of gear *B*, etc. For multi-stage transmission system, there may be several sets of parameters that satisfy the transmission ratio requirement. However, under constraint of static stiffness requirement, there may be an optimal set of parameters. Thus, sensitivity analysis is needed to provide a useful way to choose an optimal parameter set.

Rewriting Eq. (7) in the form of gear's parameters results in

$$A_{n(n+1)} = \begin{cases} \dfrac{4k_n}{4k_n + m_n^2 z_n^2 k_{(n-1)} - m_{n-1} m_n z_{(n-1)} z_n \cos^2\alpha k_{(n-1)} A_{(n-1)n}} & n = odd \\ \dfrac{m_n m_{n+1} z_n z_{n+1} \cos^2\alpha k_n}{4k_{(n-1)} + m_n^2 z_n^2 \cos^2\alpha k_n - 4k_{(n-1)} A_{(n-1)n}} & n = even \end{cases} \tag{19}$$

3.4 Sensitivity to driving gear's teeth number

By continuous differential operation, the sensitivity to driving gear's teeth number is computed as

$$\frac{\partial k_{static}}{\partial z_n} = -k_{n+1} \prod_{i=n+2}^{N} A_{i(i+1)}^2 (\mathring{A}_{n+1}(r_{bn}) \frac{\partial r_{bn}}{\partial z_n} + \mathring{A}_{n+1}(k_n) \frac{\partial k_n}{\partial z_n}) \tag{20a}$$

where $\mathring{A}_{n+1}(r_{bn}) = \dfrac{2k_n(r_{bn+1} - r_{bn}A_{n(n+1)})A_{n(n+1)}A^2_{(n+1)(n+2)}}{k_{n+1}}$,

$$\mathring{A}_{n+1}(k_n) = \frac{-(r_{bn}A_{n(n+1)} - r_{bn+1})^2 A^2_{(n+1)(n+2)}}{k_{n+1}}.$$

Similarly, the sensitivity to driven gear's teeth number is given by

$$\frac{\partial k_{static}}{\partial z_{n+1}} = -k_{n+1}\prod_{i=n+2}^{N} A^2{}_{i(i+1)}(\mathring{A}_{n+1}(r_{bn+1})\frac{\partial r_{bn+1}}{\partial z_{n+1}} + \mathring{A}_{n+1}(k_n)\frac{\partial k_n}{\partial z_{n+1}}) \tag{20b}$$

where $\mathring{A}_{n+1}(r_{bn+1}) = \dfrac{k_n(r_{bn}A_{n(n+1)} - 2r_{bn+1})A^2_{(n+1)(n+2)}}{k_{n+1}}$.

The sensitivity to gear's width is given by

$$\frac{\partial k_{static}}{\partial B_n} = -k_{n+1}\prod_{i=n+2}^{N} A^2_{i(i+1)}\mathring{A}_{n+1}(k_n)\frac{\partial k_n}{\partial B_n} \tag{20c}$$

Based on the basic formulations for gear, there are

$$\frac{\partial r_b}{\partial z} = m \cdot \cos\alpha / 2 \tag{21a}$$

$$\frac{\partial r_b}{\partial m} = z \cdot \cos\alpha / 2 \tag{21b}$$

where m, α are the module and pressure angle, respectively.

In Figure 4, the x-axis represents the meshing time for a pair of gears, and y-axis represents the meshing stiffness of the meshing gear teeth. T_{m} means the meshing period, S_m is the time interval for double teeth contact in a period. t_1, t_2, t_3 represent the change time of mesh stiffness of helical gear pairs. K_{max} denotes the maximum mesh stiffness of gear teeth, $K_{\min}$ denotes the minimum stiffness and K_{m} represents the mean value of the stiffness. Figure 4(a) shows the mesh stiffness of spur gear pair, whereas mesh stiffness of helical gear pair is shown in Figure 4(b). As shown in the figure, the mesh stiffness is periodically time-varying.

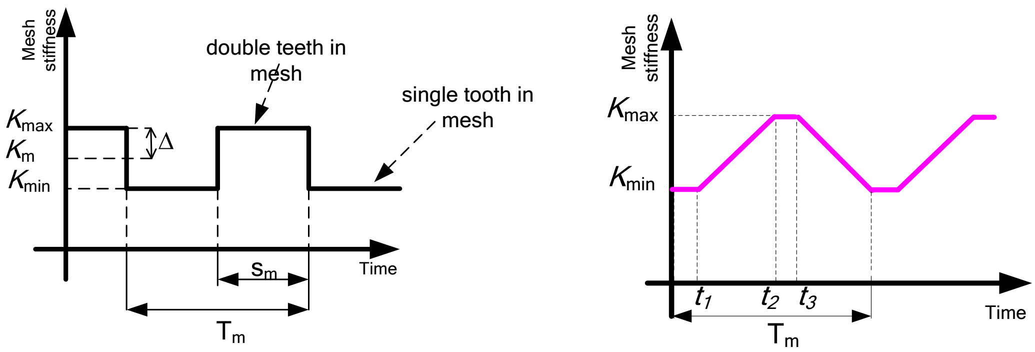

Figure 4 meshing stiffness of gear pair: (a) spur gear pair (b) helical gear pair

The stiffness usually could be expanded into Taylor's series and the *n*th mesh stiffness could be expressed as

$$k_n(t) = k_{m,n} + \Delta_n(2\varepsilon_n - 3) + \sum_{l=1}^{\infty} \frac{4\Delta_n}{l\pi} \sin[l(\varepsilon_n - 1)\pi]\cos[l\omega_m(t-\varphi)] \tag{22}$$

where ε_n is the contact ratio, ω_m is the meshing frequency, φ is phase angle . $k_{m,n} = 1.5k_{0,n}$, $\Delta_n = 0.5k_{0,n}$, $k_{0,n}$ is defined as the mean mesh stiffness of a single tooth pair and takes the following form[18]:

$$k_{0,n}(z_n, z_{n+1}, B_n) = 6400B_n / q \tag{23a}$$

where B_n is the gear width and q for gears without addendum modification is approximated by[18]

$$q = 0.04732 + 0.15551/z_1 + 0.25791/z_2 \tag{23b}$$

The contact ratio ε_n in Eq. (22) is given by

$$\varepsilon_n = \frac{1}{2\pi}[z_1(\tan\alpha_{a1} - \tan\alpha') + z_2(\tan\alpha_{a2} - \tan\alpha')] \tag{23c}$$

where α_{a1} , α_{a2} are the pressure angles at addendum of pinion and gear, respectively, α' is the pressure angle at pitch circle of gears under non-standard installation. Under standard installation, the contact ratio is only the function of teeth number.

Defining

$$L_n(z_n, z_{n+1}, t) = a_\varepsilon z_n + b_\varepsilon z_{n+1} + \frac{2}{\pi}\sum_{l=1}^{\infty}\frac{\sin[l(a_\varepsilon z_n + b_\varepsilon z_{n+1} - 1)\pi]}{l}\cos[l\omega_m(t-\varphi)] \tag{23d}$$

where $a_\varepsilon = (\tan\alpha_{an1} - \tan\alpha')/(2\pi)$, $b_\varepsilon = (\tan\alpha_{an2} - \tan\alpha')/(2\pi)$

Then the mesh stiffness for *n*th gear pair is expressed as

$$k_n(z_n, z_{n+1}, B_n, t) = L_n(z_n, z_{n+1}, t)\cdot k_{0,n}(z_n, z_{n+1}, B_n) \tag{23e}$$

Therefore, the sensitivities of mesh stiffness to teeth number, width are obtained by partial differentiating:

$$\frac{\partial k_n(z_n, z_{n+1}, B_n, t)}{\partial z_n} = (a_\varepsilon + 2a_\varepsilon\sum_{l=1}^{\infty}\cos[l(a_\varepsilon z_n + b_\varepsilon z_{n+1} - 1)\pi]\cos[l\omega_m(t-\varphi)]) \cdot k_{0,n}(z_n, z_{n+1}, B_n) + \frac{0.15551 k_{0,n}(z_n, z_{n+1}, B_n)}{q^2 z_n^2} \tag{23f}$$

$$\frac{\partial k_n(z_n, z_{n+1}, B_n, t)}{\partial z_{n+1}} = (b_\varepsilon + 2b_\varepsilon\sum_{l=1}^{\infty}\cos[l(a_\varepsilon z_n + b_\varepsilon z_{n+1} - 1)\pi]\cos[l\omega_m(t-\varphi)]) \cdot k_{0,n}(z_n, z_{n+1}, B_n) + \frac{0.25791 k_{0,n}(z_n, z_{n+1}, B_n)}{q^2 z_{n+1}^2} \tag{23g}$$

$$\frac{\partial k_n(z_n, z_{n+1}, B_n, t)}{\partial B_n} = 6400 L_n(z_n, z_{n+1}, t)/q \tag{23h}$$

Combining Eqs (21)~(23), the sensitivity of static stiffness to the gear's parameter could be found in an analytical expression form.

4. Example Study

4.1 Model verification

To verify the presented unified static stiffness model, a comparison between the proposed model and traditional model is conducted.

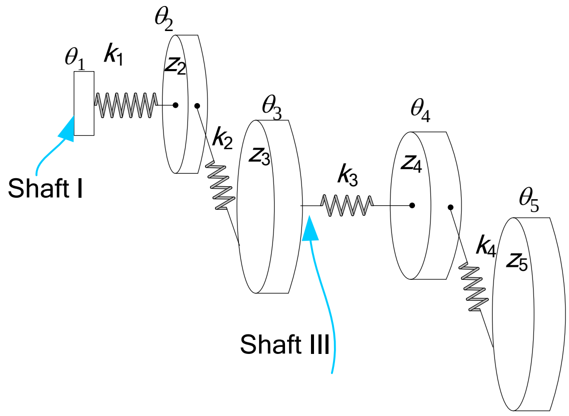

Figure 5 an example transmission system

A two-stage transmission system is shown in Figure 5. The torsional stiffnesses of shafts are denoted as k_1, k_3, respectively. Accordingly, the mesh stiffnesses of gear pairs are denoted as k_2, k_4, respectively. The system's parameters are shown in Table 1.

Table 1 parameters of the two-stage transmission system

	Gear 2	Gear 3	Gear 4	Gear 5	Shaft 1	Shaft 3
Teeth number	21	67	17	71		
Module (m)	4		5			
Width (mm)	56		66			
Pressure angle			20 °			
Speed (rpm)				1		
Radius (mm)					35	35
Length (mm)					80	80

In traditional modeling method, the system is equivalent to be a series system of springs with different stiffness values of shaft's. According to energy-equivalent principle, the static stiffness k_{eq} of the series after equivalent could be obtained as:

$$k_{eq} = \frac{1}{\frac{(z_2 z_4 / z_3 z_5)^2}{k_1} + \frac{(z_4 / z_5)^2}{k_3}}$$

Meanwhile, the static stiffness obtained by the presented method is computed as

$$k_{static} = r_{b5}^2 k_4 - r_{b4} r_{b5} k_4 A_{45}$$

where $A_{23}=\dfrac{r_{b2}r_{b3}k_2}{k_1+k_2r_{b2}^2}$, $A_{34}=\dfrac{k_3}{k_3+k_2r_{b3}^2-k_2r_{b2}r_{b3}A_{23}}$, $A_{45}=\dfrac{r_{b4}r_{b5}k_4}{k_3+k_4r_{b4}^2-k_3A_{34}}$.

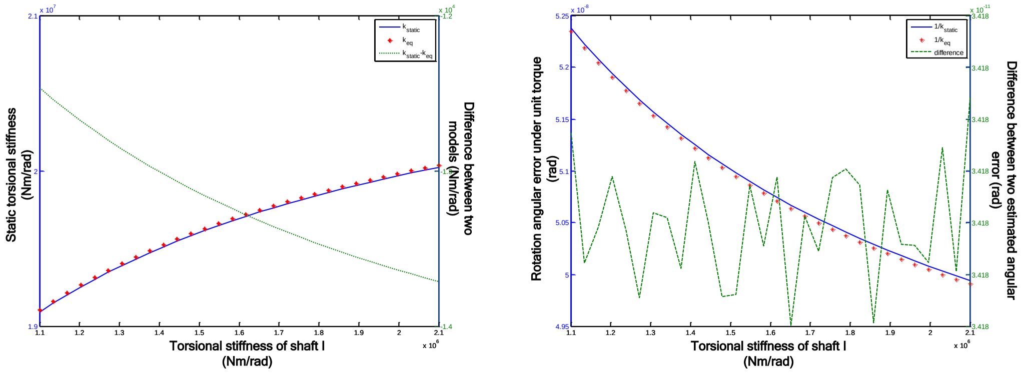

(a) (b)

Figure 6 comparison between the results from two models: (a) static stiffness (b) angular error under unit torque

The results from both models are shown in Figure 5(a), where the torsional stiffness of shaft I is taken as a variable. As could be seen from the figure 6(a), a good agreement is obtained, even though there is little difference (about 1/1000 of the estimated stiffness value) between two results which are induced by the mesh stiffness of gear pairs. It's also could be seen from the figure that the static stiffness increases with the increasing of the shaft's stiffness, however, the increasing rate becomes smaller and smaller. Obviously, similar cases could be found when stiffness of other elements is taken as a variable, as the system is equivalent to a series of springs. Figure 6(b) shows the estimations of angular errors from two models under unit torque load and the difference between the results from two models is small enough to be neglected.

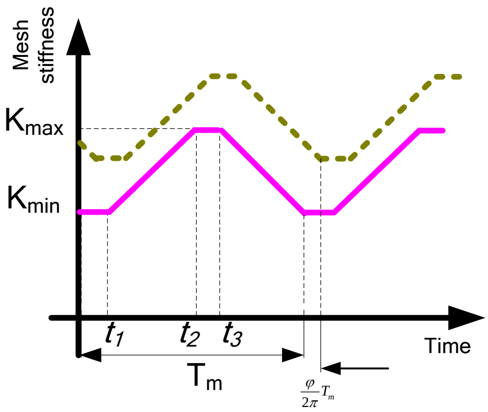

Figure 7 meshing phase angle

The phase angle for each meshing gear pair is denoted by φ. As shown in Figure 7, if the solid line is taken as the reference which means $\varphi_{solid} = 0$, then the mesh phase angle difference between two pairs is $\frac{\varphi}{2\pi} T_m$. The corresponding static stiffness of the example with different phase angles is shown in Figure 8, respectively. The *x*-axis represents the rotating time of the end gear, while the *y*-axis represents the resultant static stiffness.

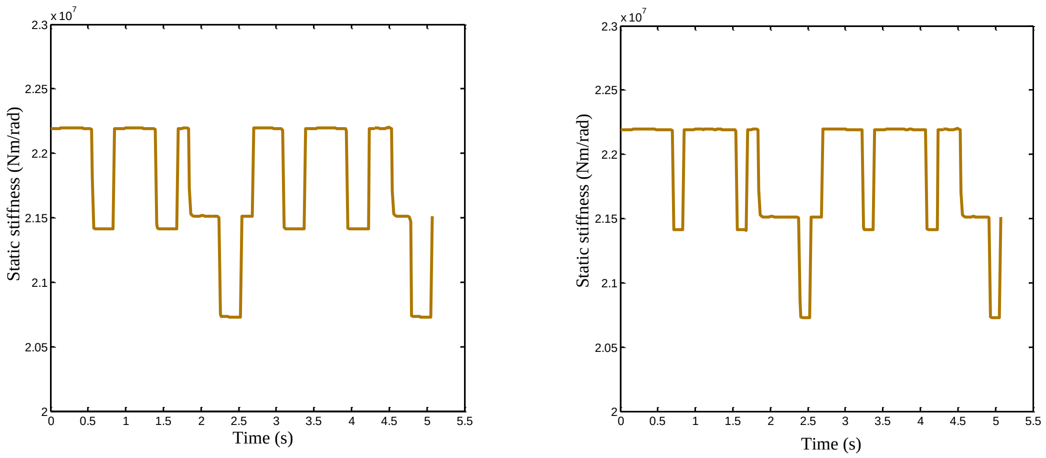

(a) $\varphi = 0^o$ (b) $\varphi = 30^o$

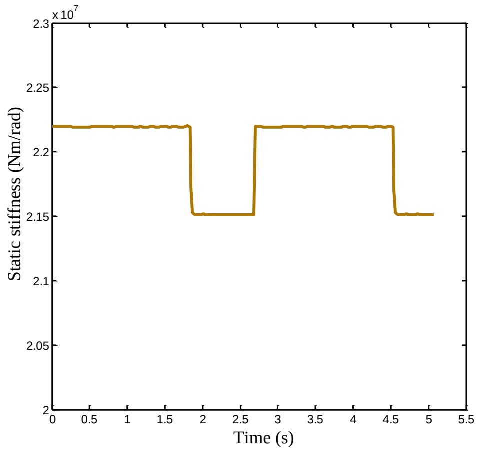

(c) $\varphi = 64^{o}$

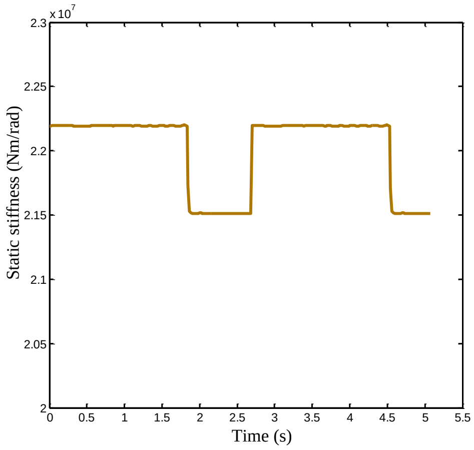

(d) $\varphi = 90^{o}$

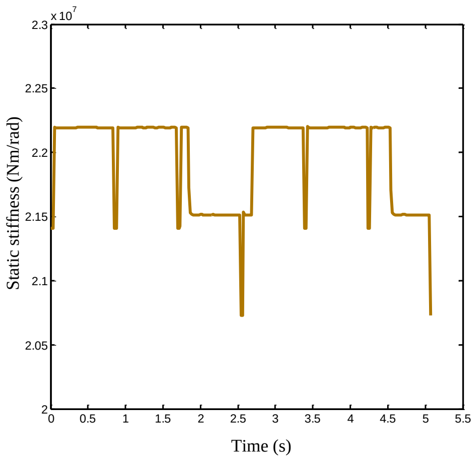

(e) $\varphi = 128^{o}$

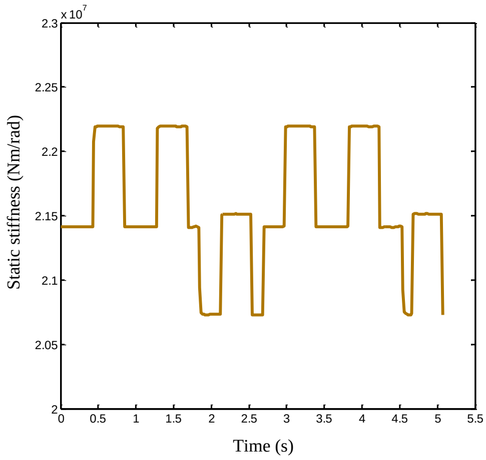

(f) $\varphi = 180^{o}$

Figure 8 static stiffness with phase angle difference

As the figure shows, the resultant static stiffness takes different extremes and frequencies under different phase angles of the two meshing pairs. Thus, the phase angle should be paid attentions to get desired profile of static stiffness. It's that the difference becomes smaller in geared system with more stages. Similar to reference [1], the mean value of the mesh stiffness of individual meshing pair is employed to conduct sensitivity analysis.

4.2 Sensitivity analysis results

The sensitivity to individual element’s stiffness is shown in Figure 9. As mentioned above, only the mean value of the mesh stiffness is considered in the simulation.

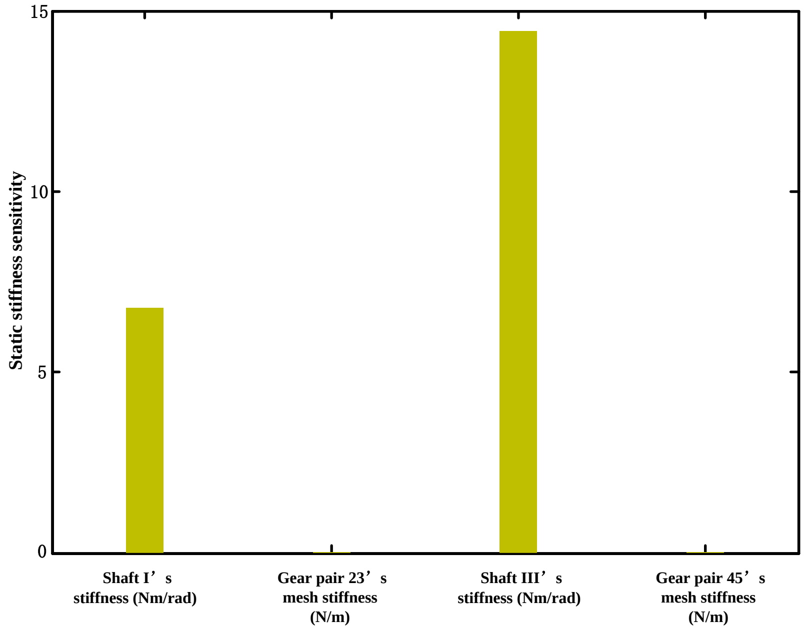

Figure 9 sensitivity to individual’s stiffness

It’s shown that the two shafts’ torsional stiffnesses are more sensitive to the equivalent static stiffness, compared to those of two gear pairs. Moreover, the second shaft’s torsional stiffness is the most sensitive one, as it’s nearer to the end worktable.

The sensitivity to teeth number is shown in Figure 10. As could be seen from the figure 10(a), the teeth numbers of gear pair nearer to the end driven gear are more sensitive to the equivalent static stiffness. In addition, the teeth number of driving gear of each gear pair is more sensitive to the static stiffness, compared with the driven gear’s one. Meanwhile, as figure 10 (b) shows, the width of the gear pair at the output shaft is more sensitive than those far away from the output shaft.

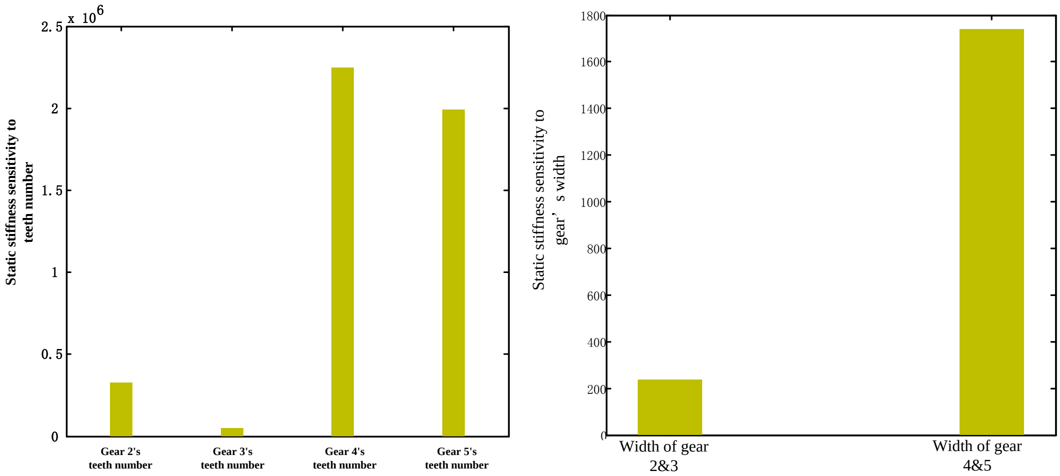

(a) (b)

Figure 10 sensitivity to teeth number and gear width

It’s known that the longer of a shaft is, the smaller of the torsional stiffness is. However, only the absolute values of sensitivity of static stiffness to the shaft’s parameters are used in the analysis.

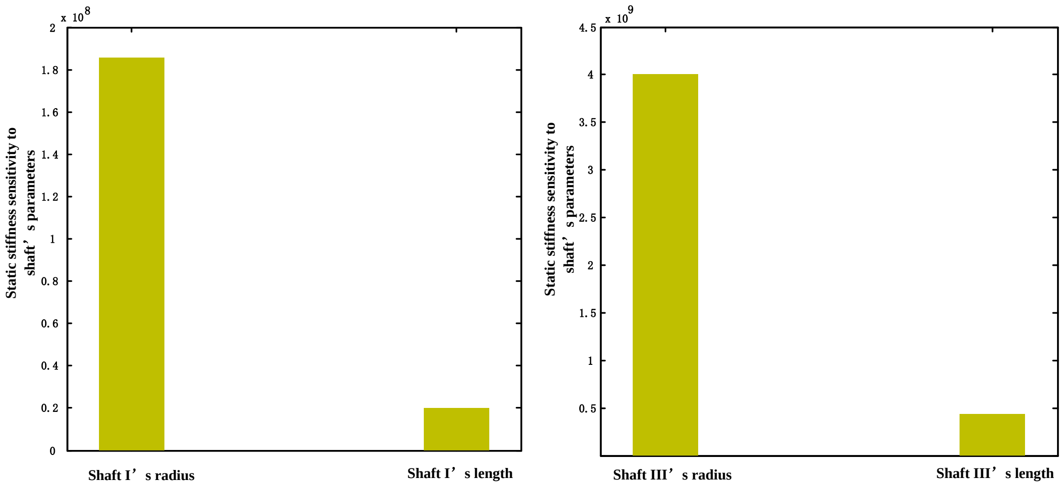

Figure 11 sensitivity to shaft’s parameters

As shown in Figure 11, the shaft’s radius is more sensitive to the static stiffness than the length of the shaft. Moreover, the sensitivity of the shaft’s parameters nearer to the end gear is more sensitive than those far away from the end gear.

5. Conclusion

This paper presented a unified static stiffness model for geared transmission system.

The analytical expressions for sensitivity of the static stiffness to individual stiffness including torsional stiffness of shaft and mesh stiffness of gear pair were derived. For the presented example transmission system, the effect of phase angle on the resultant static stiffness should not be ignored if more accurate value of stiffness is desired. Furthermore, the sensitivity of static stiffness to the geared system's design parameters was also explored. Following conclusions could be reached:

1) the influence of gear pair' mesh stiffness on the equivalent stiffness is less significant than those of the shafts in the geared system;

2) the radius of a shaft is more sensitive to the static stiffness than the length of the shaft;

3) the teeth number of driving gear is more sensitive than the driven gear's, similar conclusion could be made about the gear's width.

The presented model and sensitivity analysis provides an essential tool for further performance improvement of geared transmission chain. Future work will focus on: a) the optimization of design parameters to minimize the chain's volume, b) stiffness matching designs for a transmission chain, where the static stiffness will be dealt as a constraint or an objective.

Acknowledgement

This work was supported by the National High Technology Research and Development Program of China (Grant No. 2012AA040701).

Reference

1. Wu, Z., Liu, H., Yuan, D., et al. A study of analysis and experiment on transmission

stiffness of the transverse feed system of a type of heavy duty lathe. *Journal of Experimental Mechanics* 2011; 26:457-463.

2. Ebrahimi M, Whalley R. Analysis. Modeling and simulation of stiffness in machine tool drives. *Comput Ind Eng* 2000; 38:93-105.

3. Kim, M. and Chung, S. Integrated design methodology of ball-screw driven servomechanisms with discrete controllers. Part I: Modeling and performance analysis. *Mechatronics* 2006; 16:491-502.

4. Lei, W.T. M.P. Sung, et al. Double ballbar test for the rotary axes of five-axis CNC machine tools. *Int J Mach Tool Manu* 2007; 47:273-285.

5. K.M.Muditha Dassanayake, Masaomi TSUTSUMI, Ryuta SATO, et al. Motion characteristics of high performance rotary tables for cnc machines. *ASME International Mechanical Engineering Congress and Exposition*, Oct. 31~Nov.6, 2008, Boston, Massachusetts, USA.

6. Hong, C., Ibaraki, S. and Matsubara, A. Influence of position-dependent geometric errors of rotary axes on a machining test of cone frustum by five-axis machine tools. *Precis Eng* 2011; 35:1-11.

7. Hong, C. and Ibaraki, S. Observation of thermal influence on error motions of rotary axes on a five-axis machine tool by static R-test, *International Journal of Automation Technology* 2012; 6(2):196-204.

8. Ibaraki, S., Oyama, C., Otsubo., H.. Construction of an error map of rotary axes on a five-axis machining center by static R-test. *Int J Mach Tool Manu* 2011; 51(3):190-200.

9. Ibaraki, S., Iritani, T., Matsushita, T.. Error map construction for rotary axes on five-axis machine tools by on-the-machine measurement using a touch-trigger probe. *Int J Mach Tool Manu* 2013; 68: 21-29.

10. Lee, K., Lee, D.M., Yang, S.H.. Parametric modeling and estimation of geometric errors for a rotary axis using double ball-bar. *Int J Adv Manuf Tech* 2012; 62(5-8):741-750.

11. Lee, K., Yang, S.H.. Robust measurement method and uncertainty analysis for position-independent geometric errors of a rotary axis using a double ball-bar. *Int J Precis Eng Man* 2013; 14(2):231-239.

12. Lysov M.S., Starikov A.V.. Mathematical model of rotary table in control problems, *Russian Engineering Research* 2009; 29:719-722.

13. Ryuta SATO. Mathematical model of CNC rotary table driven by worm gear. *The 15th ICMT*, Melbourne, Victoria, Australia, 30 Nov-2 Dec 2011.

14. F Zhao, X Mei, T Tao, G Jiang, Y Zhou. Fault diagnosis of a machine tool rotary axis based on a motor current test and the ensemble empirical mode decomposition method. *Proc IMechE Part C: J Mech Eng* 2011; 225(5): 1121-1129.

15. Yu, C., Huang, X. And Fang, C. Research on dynamic characteristics of NC rotary table considering leakage factors of its hydrostatic guideway, *Proc IMechE Part C: J Mech Eng* 2012; 226(11):2674-2685.

16. Yu, C., Huang, X. And Fang, C. Optimizing dynamic characteristics of NC rotary table based on electromechanical-hydraulic coupling, *J Mech Sci Technol* 2013; 27(4):1081-1088.

17. Feng, H. and Jiang, S. Multicriteria design of a rotary table with a hybrid constant flow and constant pressure supply system, *Proc IMechE Part J: J Eng Tri* 2013; 0(0):1-12. DOI: 10.1177/1350650113483053.

18. Liu., Z. Research on dynamic characteristics of vehicle compound planetary gear train sets, Doctorial dissertation, Wuhan: Wuhan University, 2012.

Appendix

notation

a_ε	auxiliary parameter	r_{bi}	radius of basis circle of i^{th} gear
$A_{n(n+1)}$	auxiliary parameter	$r_n^{(i)}$	radius of i^{th} section of n^{th} shaft
b_ε	auxiliary parameter	S_m	time interval for double teeth contact
B_n	gear width	S_n	number of sections of n^{th} shaft
c_i	damping coefficient	t_1, t_2, t_3	different mesh time instant
D_n	auxiliary parameter	T_1	driving torque
E	Young modulus	T_L	load torque
G	$=0.5E/(1+v)$	T_m	meshing period
$H_n^{(j)}$	auxiliary parameter	z_n	tooth number of n^{th} gear
i_{total}	transmission ratio		
J_i	inertia of i^{th} gear	α	pressure angle
$J^{(i)}$	polar moment of inertia	α'	pressure angle at pitch circle
$k_{0,n}$	mean stiffness of single tooth	α_{a1}	pressure angle at addendum of pinion
k_i	individual stiffness	α_{a2}	pressure angle at addendum of gear
k_{static}	static stiffness	Δ_n	auxiliary parameter
K_m	mean value of mesh stiffness	$\Delta\theta$	angular error
K_{max}	maximum mesh stiffness	ε_n	contact ratio of n^{th} gear pair
K_{min}	minimum mesh stiffness	θ_i	rotating angle
$L^{(i)}$	length of shaft	v	Poisson coefficient
L_n	auxiliary parameter	φ	phase angle
m_n	modulus of n^{th} gear	ω_m	meshing frequency
q	auxiliary parameter		
q_n	auxiliary parameter		